Cell

Toxoplasma gondii Sequesters Lysosomes from Mammalian Hosts in the Vacuolar Space

Isabelle Coppens,[1,*] Joe Dan Dunn,[2] Julia D. Romano,[1] Marc Pypaert,[3] Hui Zhang,[1] John C. Boothroyd,[2] and Keith A. Joiner[4]
[1] Department of Molecular Microbiology and Immunology, Johns Hopkins University Bloomberg School of Public Health, 615 N. Wolfe Street, Baltimore, MD 21205, USA
[2] Department of Microbiology and Immunology, Stanford University School of Medicine, 299 Campus Drive, Stanford, CA 94305, USA
[3] Department of Cell Biology, Yale University School of Medicine, 333 Cedar Street, New Haven, CT 06520, USA
[4] Arizona Health Science Center, University of Arizona, College of Medicine, 1501 N. Campbell Avenue, Tucson, AZ 85724, USA
*Contact: icoppens@jhsph.edu
DOI 10.1016/j.cell.2006.01.056

SUMMARY

The intracellular compartment harboring *Toxoplasma gondii* satisfies the parasite's nutritional needs for rapid growth in mammalian cells. We demonstrate that the parasitophorous vacuole (PV) of *T. gondii* accumulates material coming from the host mammalian cell via the exploitation of the host endo-lysosomal system. The parasite actively recruits host microtubules, resulting in selective attraction of endo-lysosomes to the PV. Microtubule-based invaginations of the PV membrane serve as conduits for the delivery of host endo-lysosomes within the PV. These tubular conduits are decorated by a parasite coat, including the tubulogenic protein GRA7, which acts like a garrote that sequesters host endocytic organelles in the vacuolar space. These data define an unanticipated process allowing the parasite intimate and concentrated access to a diverse range of low molecular weight components produced by the endo-lysosomal system. More generally, they identify a unique mechanism for unidirectional transport and sequestration of host organelles.

INTRODUCTION

Obligate intracellular pathogens include a special category of microorganisms that must live within cells in order to survive. By entering into the confines of a host cell, these pathogens assure a ready source of nutrients and protection from immune confrontations. Living like an obligate intracellular pathogen is taken as *prima facie* evidence that the microorganism must acquire, from inside the host cell, the nutrients that cannot be obtained at a sufficient rate from the external medium.

There are a limited number of strategies by which intracellular pathogens can divert host nutrients. Such mechanisms depend, in part, on the intracellular locale in which the organism resides in mammalian cells. For pathogens living freely in the host cytosol, diffusion and/or transport of host molecules across the microbial outer/plasma membranes or endocytosis of macromolecules from the host cytosol can occur. For pathogens residing intracellularly in host endocytic compartments, fusion of host endocytic organelles with the pathogen vacuole can deliver contents to the vacuolar space, from where they can be taken up by the mechanisms described above.

The most enigmatic situation exists with pathogens living in a vacuole which does not intersect the host cell endocytic pathway. One such organism is *Toxoplasma gondii*, a member of the apicomplexan family. Infections with *T. gondii* are extremely common, but disease only develops in immunocompromised and immunologically immature individuals (Hall et al., 2001). *T. gondii* is adapted to thrive in a unique, self-made niche, i.e., the parasitophorous vacuole (PV), within the cytoplasm of a large variety of mammalian cells. Upon invasion, the parasite actively excludes many host membrane proteins from the PV membrane (PVM) and further inserts novel proteins from its secretory organelles, the rhoptries, and the dense granules (Joiner and Roos, 2002). These coordinated events confer unusual biochemical and biophysical properties on the PVM, creating a nonfusogenic vacuole and securing parasites in a locale isolated from the host cell vesicular transport system.

Such segregation of the PV from host cell endocytic or exocytic pathways negates the possibility of acquisition of proteins or lipids whose trafficking is restricted to those pathways. This suggests that the needed host components must be selectively mobilized via nonvesicular

transport routes, or unconventional pathways. Yet secluded in its niche, *Toxoplasma* has the ability to modify PVM permeability to allow free diffusion of small molecules, e.g., sugars, amino acids, nucleobases, and cofactors from the host cytoplasm, to the vacuolar space (Schwab et al., 1994). *T. gondii* may also gain access to potential sources of lipids by recruiting host mitochondria and endoplasmic reticulum (ER), the cell lipid biosynthetic apparatus (Sinai et al., 1997), to its PV.

Unequivocally, *T. gondii* must acquire cholesterol from the host cell (Coppens et al., 2000). Our previous work demonstrated that the parasite diverts low-density lipoprotein (LDL)-derived cholesterol through host LDL receptor-mediated endocytosis. The absence of fusion between host endocytic compartments and the PV suggests, speculatively, that LDL cholesterol might be transported through the host cell to the PVM by cholesterol transport proteins. From that destination, it has been suggested that an extensive collection of elongated nanotubules forming a tubulo-vesicular network (TVN) in the vacuolar space might participate in delivering nutrients from the PVM to the parasite (Sibley et al., 1995). Indeed, this membrane network appears fused at points with the PVM, providing a potential physical connection for lipid traffic from the PVM to the vacuolar space, and potentially to the parasite, or the reverse (Lingelbach and Joiner, 1998).

We resolve this speculation, in unexpected fashion. We show here that host endocytic structures are translocated along host microtubules (MTs) to the PV and delivered intact into the vacuolar space by MT-based invaginations of the PVM. The tubules mediating the vesicle delivery system are then stabilized by the formation of a protein coat of parasite origin. On one hand, this elaborate process dramatically accentuates parasite access to a diverse range of low molecular weight components from host digestive compartments sequestered in the PV. On the other hand, these results refute the previous dogma asserting complete seclusion of the *Toxoplasma*-containing vacuole from host endo-lysosomal pathways.

RESULTS

Host Endo-Lysosomes Are Gathered around the PV in the Perinuclear Area

Our previous experiments demonstrated a rapid and nearly complete transfer of LDL-derived cholesterol from host endocytic organelles to the PV of *Toxoplasma gondii* (Coppens et al., 2000). This surprising observation implied that some mechanisms led to the diversion and sequestration of material from the host endocytic compartments to intracellular parasites. We probed this possibility, by assessing the distribution of host endocytic compartments in *T. gondii*-infected cells using three separate and independent approaches (Figures 1, 2, and S1): (1) LysoTracker-containing organelles (Figure 1A); (2) endocytic structures loaded with LDL then stained with the fluorescent sterol binding dye filipin (Figure 1B), with LDL-gold particles (Figure 1F) or with Texas red-epidermal growth factor (EGF) (Figure 2C); and (3) Lamp1 (Lysosome-associated membrane protein 1)-labeled organelles (Figures 1D and 1E). Findings were concordant from all these approaches, illustrating the host endo-lysosome concentration primarily to the perinuclear region. After 2 hr of infection (Figure 1C), 19% of the total host cell LysoTracker-containing structures clustered around the PV, increasing to 73% by 48 hr post-infection (p.i.).

Host MTs Are Reorganized around the PV

A major role for interphase MTs is to support the membrane vesicle movements involved in cellular membrane trafficking. We therefore questioned whether the striking tropism of host endocytic structures to the *Toxoplasma* PV involved host MTs. Remarkable changes in host MT-organizing center (MTOC) localization and MT morphology were visible in infected cells (Figures 2A and S2). Host MTOC were detached from the nuclear envelope and associated with the PV. Live-cell imaging of infected PtK2 cells expressing fluorescent α-tubulin illustrated that MTs were specifically concentrated around each individual PV (Figure 2B). This contrasted with MTs in uninfected cells, which formed a framework surrounding the nucleus, radiating toward the cell periphery. Individual MTs surrounding small PV were shrunken and shortened compared to MTs located in the host cytoplasm. MT overcoating of the PV was initiated 4 to 6 hr p.i., and mature PV were completely encaged by the network of host MTs after 24 hr p.i.

The relationship of the PV to the MT network was probed using taxol, to interfere with the dynamics of the microtubular network. When infected cells were exposed to taxol prior to Texas red-EGF incubation, vesicles were predominantly restricted to the cell periphery (as observed in uninfected cells), resulting in negligible labeling around the PV (Figure 2C). At the ultrastructural level, taxol treatment of host cells revealed an extensive array of host MTs closely apposed to the PVM, regularly spaced at 15 nm from one another (Figure 2D). Under physiological conditions, some profiles illustrated deep invaginations of the PVM (up to 1.2 μm in length) into the lumen of the vacuole (Figures 2E and S3). These invaginations always contained a central host MT, implying a dynamic interaction between host MTs and the PV. The host MT remodeling is specific to *Toxoplasma* infection since mammalian cells harboring other apicomplexan parasites (e.g., *Neospora caninum*; Figure S2) did not show any alterations in the MT cytoskeleton organization under parasite assault.

The host MT bundles clearly codistributed with vimentin intermediate filaments around the PV (Figure S2; Halonen and Weidner, 1994), while the distribution of host actin microfilaments remained unchanged. Host Golgi, normally positioned in the perinuclear region by centrosomal MTs, was found fragmented into smaller units at the PV surface (Figure S2). By contrast, host peroxisomes remained scattered in the host cytoplasm (Figure S2).

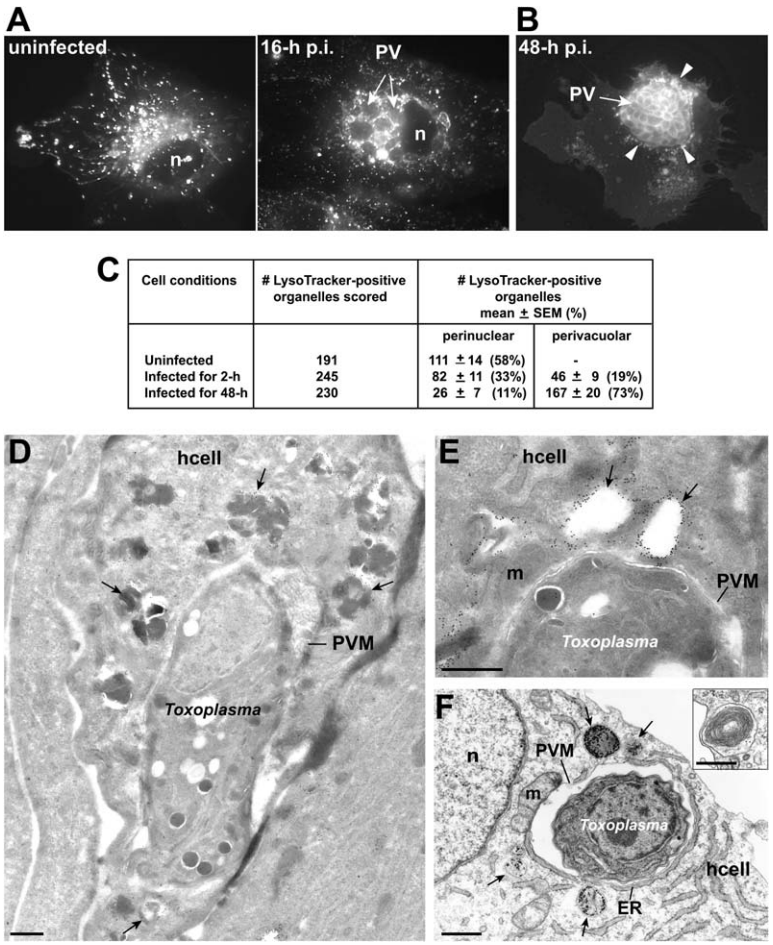

Cell conditions	# LysoTracker-positive organelles scored	# LysoTracker-positive organelles mean ± SEM (%)	
		perinuclear	perivacuolar
Uninfected	191	111 ±14 (58%)	-
Infected for 2-h	245	82 ±11 (33%)	46 ± 9 (19%)
Infected for 48-h	230	26 ± 7 (11%)	167 ± 20 (73%)

Figure 1. Association of Host Endo-Lysosomes with the PV

(A and B) Fluorescence microscopy showing the distribution of LysoTracker-containing organelles in uninfected VERO cells (left panel) or infected for 16 hr (middle panel) (A) or filipin-labeled compartments (arrowheads) in a VERO cell infected for 48 hr and incubated with 2 mg/ml of LDL (B).

(C) Quantitation of average host LysoTracker-positive organelles and PV positions in infected and uninfected cells.

(D and E) Immunogold labeling of infected cells using anti-Lamp1 antibodies followed by incubation with protein A adsorbed to 10 nm gold particles. Arrows are pointing to the Lamp1-positive structures.

(F) Transmission EM (TEM) of *Toxoplasma*-infected VERO cells incubated with LDL-gold particles for 5 min, illustrating LDL-gold-loaded organelles (arrows) around a PV. A close apposition of a host-labeled structure to the PVM is visible in the inset.

Bars are 0.5 μm. hcell, host cell; m, mitochondrion; n, nucleus.

Host Endocytic Structures Are Ultimately Trapped within the PV

The interaction between host endocytic compartments and MTs in proximity to the PV was examined by electron microscopy (EM) using LDL adsorbed to colloidal gold particles to obtain a substantial staining of organelles along the endocytic pathway (Figures 3, S4, and S5). Numerous gold-containing structures were distributed around the PV, often associated with MTs, or in direct contact with the PVM (Figures 3A and 3B), with protrusion of this membrane into the vacuolar space. Astonishingly, several gold-containing structures were noticed in the lumen of the PV after 30 min of incubation with LDL-gold (Figure 3C). These structures were always surrounded by a continuous membrane that was derived from the PVM, as demonstrated below. No free gold particles were ever seen inside the PV, corroborating the absence of fusion of host vesicles with the PVM. For comparative purposes, using the same experimental approach in cells infected with the parasite *Leishmania* residing in a compartment that fuses with endocytic organelles (Russell, 1995), free gold particles were found prominently within the PV (Figure 3D). The occurrence of host endocytic structures in the *T. gondii* PV was confirmed by ultrastructural detection of Lamp1-containing structures (Figure 3E). Determination of the proportion of sections in which Lamp1-containing structures were found in the PV lumen revealed the presence of 1.4 ± 0.5 (mean ± SEM; n = 3 separate experiments) profiles of Lamp1-positive structures per PV (Figure S4). Serial ultrathin sections of typical young or mature PV confirmed the multiplicity of LDL-containing structures close to host microtubules in the PV. Additionally, this striking presence of host endo-lysosomes in the *T. gondii* PV was commonly observed in a large variety of cell types and lines, including primary fibroblasts, epithelial cells, hepatoma cells, and macrophages, and with different labeled tracers including LDL, high-density lipoprotein, albumin, and transferrin (left inset in Figure 3C; Figure S5). In conclusion, endocytic vesicles and tracers are delivered into the PV space, but indiscriminately.

Host Endocytic Structures Are Directionally Delivered from the Host Cytoplasm to the PV

The processes required for delivery of host endo-lysosomes to the PV were next explored (Table S1). The percent of host LDL-gold-labeled structures closely associated with the PV or in the PV lumen was directly

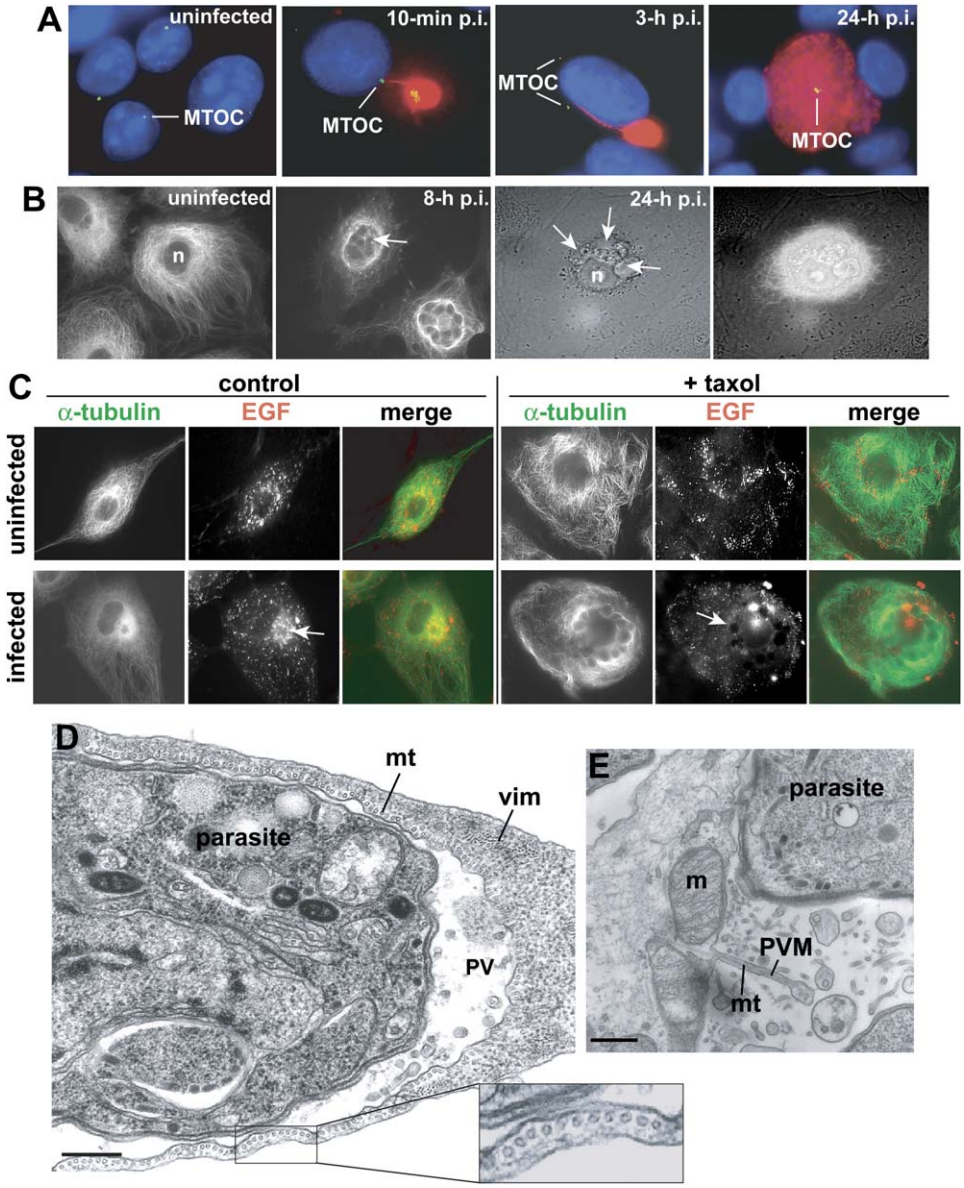

Figure 2. Host Cytosketetal Reorganization in *Toxoplasma*-Infected Cells

(A) Immunofluorescence microscopy of infected VERO cells showing PVM protrusions toward the host MTOC and the MTOC-PVM anchorage. PVM and MTOC were stained with Alexa594-labeled anti-GRA7 rabbit IgG and Alexa488-labeled anti-γ-tubulin mouse IgG, respectively.

(B) Fluorescence microscopy of YFP-α-tubulin-expressing PtK2 cells showing the microtubular network organization in (un)infected cells. Arrows pinpoint the PV. n, nucleus.

(C) Fluorescence microscopy of host MTs and endocytic structures. In control experiments, uninfected or 12-hr-infected YFP-α-tubulin-expressing PtK2 cells were incubated with Texas red-EGF. To alter MT function, cells were incubated with 4 μM taxol for 150 min prior to the addition of Texas red-EGF. For better illustration of the fluorescence pattern, a singly infected cell and a multiply infected cell were selected for control and drug treatment conditions, respectively. Arrows pinpoint the PV.

(D and E) TEM of infected HFF illustrating the corset of host MTs around the PV. In (D), an infected cell was taxol-treated (1 μM, 3 hr) to accentuate the normal MT basket beneath the PVM (see inset). In (E), a longitudinal section illustrating a PVM invagination into the vacuolar space with a central host MT is shown.

Bars are 0.25 μm. mt, host microtubule; m, mitochondrion; n, nucleus; vim, vimentin.

proportional to the infection time and increased with the vacuole surface area. When infected cells were incubated with LDL-gold particles for 10 min, before blockade of host MT function with taxol, labeled structures were seen closely apposed to the PVM but never delivered inside the PV (Figures 3F and S5). Hence, normal MT function is required for transport. In contrast, there was no alteration in the spatial distribution of host endocytic

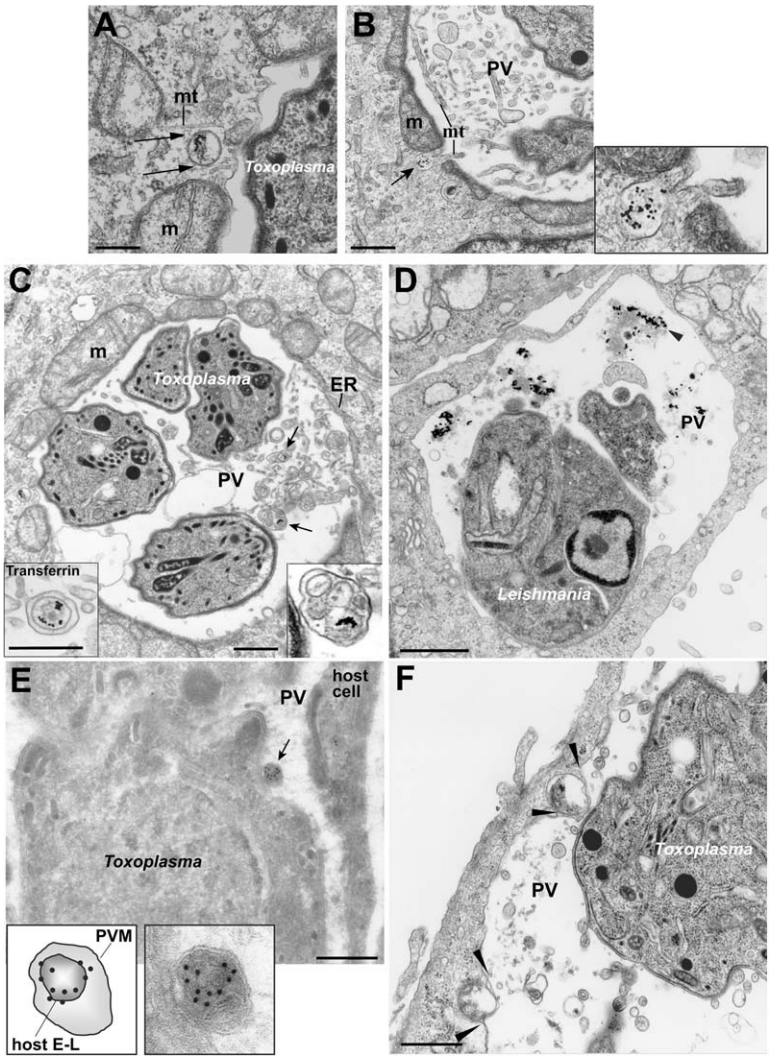

Figure 3. Ultrastructural Interaction between LDL-Gold-Labeled Endocytic Structures and the PV

(A–D) TEM of *Toxoplasma*- or *Leishmania*-infected VERO cells illustrating LDL-gold organelle distribution. Infected cells were incubated in the presence of LDL-gold particles for 15 min (A and B) or 30 min (C and D) before preparation for EM. Arrows pinpoint host LDL-containing endo- or lysosomal structures in *Toxoplasma*-infected cells (A–C). Left inset in (C) shows a PV after incubation with transferrin-gold particles for 15 min. Arrowhead shows free gold in the *Leishmania* PV (D).

(E) Immunogold labeling of *Toxoplasma*-infected cells with anti-Lamp1 antibodies followed by incubation with protein A 10 nm gold particles, demonstrating the presence of a host late endocytic organelle (arrow) within the PV. A schematic representation of the inset is shown. E-L, endo-lysosome.

(F) TEM of a *Toxoplasma*-infected VERO cell incubated with LDL-gold particles for 15 min before treatment with 4 μM taxol for 60 min before fixation, showing endocytic structures (arrowheads) protruding to but not into the PV.

Bars are 200 nm. mt, host microtubule; m, mitochondrion.

structures in infected vimentin-minus cells compared to wild-type fibroblasts.

Normal host lysosomal motility and morphology were also implicated. Nieman Pick type C (NPC) cells contain voluminous, lipid-engorged lysosome-like structures with limited intracellular motility due to impaired translocation along MTs (Lange et al., 2002). LDL-gold-labeled structures were dispersed randomly in the cytoplasm in infected NPC cells and were rarely seen in close proximity to the PV (Figure S5). Other treatments interfering with lysosomal size and motility—such as in progesterone-treated cells, chloroquine-treated cells—or inducing lysosomal retention at the cell periphery—such as extracellular acidosis, low cytoplasmic pH, or disrupting of the host MT network—also blocked the accumulation of labeled organelles at the PVM (Table S1).

Based on the above results, we hypothesize that host endocytic structures are directionally delivered from the host cytoplasm to the PV lumen using conduits formed by PVM invaginations mediated by MTs. This assertion was based on EM observations showing (1) multiple protrusions of the PVM containing a central host MT (Figures 2E, 3B, S3, 4B, and 4C) and (2) vesicles within the PV, which are either bound to the MT or accumulated at the distal end of the PVM invagination (Figure 4B). The external membrane of these tubular conduits was derived from the PVM, as demonstrated by immunoEM using antibodies against different PVM markers (Figure 4D). In the vacuolar space, numerous spherical structures containing vesicles and resembling the extremity of microtubular invaginations, were positively labeled for dense granule organelle proteins (GRA) (Figures 4D and 4E), confirming the presence of PVM invaginations into the vacuolar space. We have designated these dynamic protrusions H.O.S.T. for *H*ost *O*rganelle-*S*equestering *T*ubulo-structures.

MT-Based Invaginations of the PVM Are Decorated by Transverse Coated Striations on Their Surface

We sought to determine the mechanism for formation and stabilization of H.O.S.T. A clue came from higher

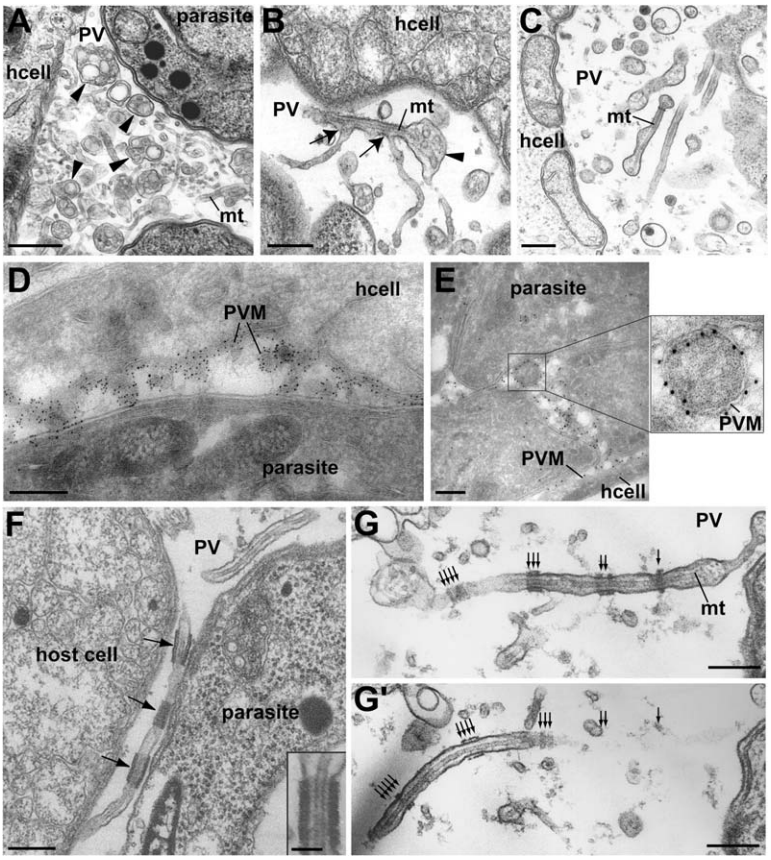

Figure 4. Ultrastructural Details of H.O.S.T. within the PVM

(A–C) TEM of MT-based invaginations in transverse (A) or longitudinal (B and C) sections. Arrowheads pinpoint the extremity of a microtubular extension sequestering organelles delivered from host cytoplasm to the PV and containing a central host MT (mt). Arrows show some tubules (probably derived from the TVN) connected to these extensions.

(D and E) Immunogold labeling of infected cells. Cryosections were incubated with anti-GRA3 (D) or -GRA7 (E) antibodies, followed by incubation with protein A adsorbed to 10 nm gold particles.

(F and G) TEM illustrating the electron dense coat (arrows) regularly organized on H.O.S.T. Inset in (F) shows a detailed transverse section of the coat. Pictures in (G)–(G′) represent serial sections of the same H.O.S.T. revealing their ramification in the PV and association with at least five coated structures constricting their diameter.

Bars are 150 nm, except 50 nm for the inset in (F). hcell, host cell.

magnification TEM, showing transverse coated striations periodically organized along the length of individual H.O.S.T. (Figures 4F, 4G, 4G′, and S6). These coated striations were 20–25 nm thick, regularly spaced, abundant, and associated with a local constriction of H.O.S.T. While this is morphologically reminiscent of the collars induced by some dynamin-like proteins (Praefcke and McMahon, 2004) mediating constriction of membranous tubules, H.O.S.T. constriction by the transverse coated striations was moderate. Indeed, the PVM was never seen in direct physical contact with the central MT but was invariably separated by ~15–20 nm and with a diameter of a coated H.O.S.T. varying between 95 to 115 nm.

Proteins Secreted by *Toxoplasma* Can Directly Bind and Deform Lipid Bilayers

Experiments were devised to determine the composition of the striated coat as well as its relationship to the formation or stabilization of H.O.S.T. The active participation of parasites was implicated since treatment of infected cells with pyrimethamine, to kill *T. gondii*, blocked trapping of labeled organelles inside the vacuole (Table S1) but not delivery to sites adjacent to the PVM. Intravacuolar *T. gondii* secretes massive amounts of proteins from dense granule organelles into the vacuolar space (Mercier et al., 2005). The predicted sequences of GRA show no homology with known tubulogenic proteins. However, GRA2 has amphiphathic α-helical domains, and GRA3 through GRA9 have hydrophobic membrane segments. All may interact with lipid bilayers as transmembrane domains, albeit with unusual characteristics. Indeed, GRA are constitutively secreted as soluble proteins and are then modified after exocytosis, allowing their association with the PVM and the TVN.

We evaluated the propensity of proteins secreted by *T. gondii* to associate with lipid bilayers and remodel membranes in vitro, as documented for tubulogenic proteins (Farsad and De Camilli, 2003). Secreted fractions (Figure 5Aa) were collected from axenic parasites and incubated with large synthetic protein-free liposomes (Figure 5Ab) as a source of membranes, before EM negative staining. *T. gondii* secreted material constricted the liposomes into long, often branched tubules (Figure 5Ac) (outer diameter between ~22 nm), resembling those generated by endophilin (Figure 5Af) (mean outer diameters ~25 nm; Farsad et al., 2001). Higher magnification micrographs revealed that the tubulated lipid structures were electron dense in the central core (Figure 5Ad). Discrete transverse constrictions were apparent along the membranes (Figure 5Ae) although thick coated striations could not be resolved. These observations represent the first evidence that material secreted by *T. gondii* can bind directly to lipid bilayers and reconfigure them into high-curvature membranes in vitro.

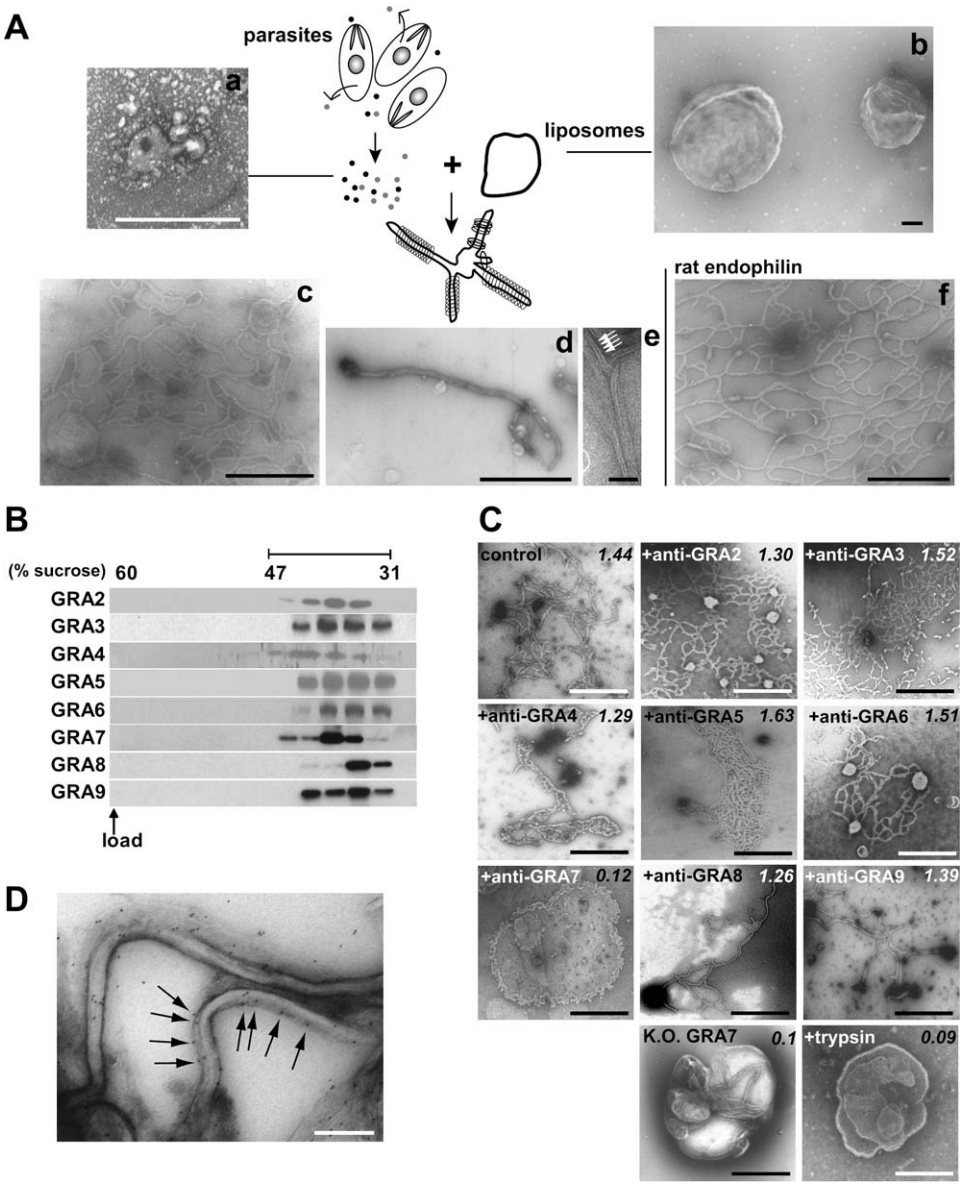

Figure 5. Tubulation of Protein-Free Liposomes by Parasite Secreted Material

(A) Negatively stained liposomes seen by TEM after incubation with parasite-secreted material (a) compared to rat endophilin. Large spherical liposomes (b) were incubated in the presence of a mixture of parasite-secreted material (c–e) or rat endophilin (f) for 20 min at 37°C with no added nucleotide. Arrows in (e) show striations.

Bars are 10 nm in (a) and (e); 100 nm in (d); and 300 nm in (b), (c), and (d).

(B) Identification of proteins associated with liposomes. After incubation with a mixture of parasite-secreted material, liposomes were purified by floatation, followed by Western blotting. GRA bound to liposomes were mainly recovered in fractions between 47%–31% sucrose gradient.

(C) Negatively stained liposomes after incubation with parasite-secreted material after GRA immunodepletion. Parasite-secreted material without treatment (*control*), immunodepleted of GRA (+ *anti-GRA2 through GRA9* antibodies), or treated with 0.25% (w/v) trypsin for 10 min (+ *trypsin*) were exposed to liposomes at 37°C for 1 hr. Tubulation intensity was quantified for each liposomal preparation. Numeric values (top right) represent light scattering values, expressed as arbitrary units after subtraction of values with liposomes alone. Trypsinization of material secreted by *T. gondii* abolished liposome tubulation, confirming the implication of parasite proteins in this process. Depletion of GRA7 but not of other GRA abolished tubulation. This result was confirmed by the inability of secreted material from the GRA7 KO to tubulate liposomes. Scale bars are 0.5 μm.

(D) Immunogold labeling of liposomes. After the liposome tubulation assay using total secreted material for 30 min at 37°C, samples were cryosectioned and incubated with anti-GRA7 antibodies, followed by addition of protein A 10 nm gold particles.

Scale bar is 100 nm.

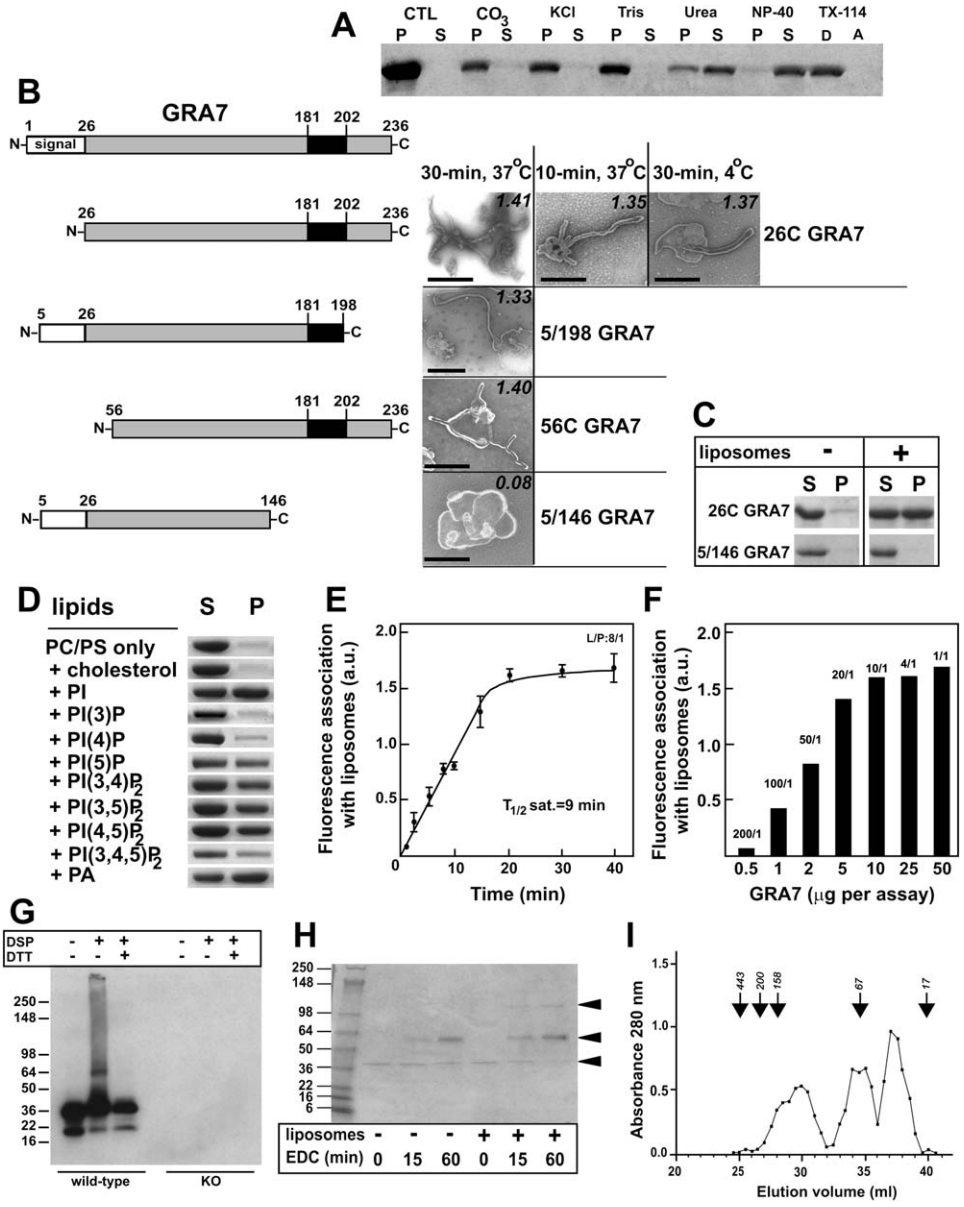

Figure 6. Demonstration of Properties of Lipid Binding and Tubulogenicity of GRA7

(A) Characterization of GRA7 association with liposomes. Liposomes containing native GRA7 were treated with various agents and separated into a soluble (S, 100,000 × *g* supernatant) and a membrane-associated pellet (P, 100,000 × *g* pellet). Fractions were analyzed by SDS-PAGE and Western blotting with anti-GRA7 antibodies.

(B) Negatively stained liposomes after incubation with mature GRA7 or recombinant GRA7 fragments. Top: schematic representation of full-length GRA7 showing the signal sequence (white) and the hydrophobic domain (black). Liposomes were incubated with the secreted native GRA7 (26C) lacking the signal sequence or with C-truncated forms of GRA7 lacking the C-terminal 38 residues (5/198 GRA7), the C-terminal 90 residues including the hydrophobic domain (5/146 GRA7), or with an N-truncated form of GRA7 lacking the signal sequence and an additional 30 residues (56C GRA7), under the indicated conditions. Tubulation intensity was monitored as described in Figure 5C.

Bars are 0.5 μm.

(C) Liposome sedimentation assays. Purified 26C GRA7 or recombinant 5/146 GRA7 were incubated with or without liposomes. The mixtures were centrifuged to pellet membrane-associated protein and then visualized by Coomassie-stained SDS-PAGE. S, supernatant; P, pellet.

(D) Liposome-26C GRA7 sedimentation assays. The indicated lipids were tested for binding to full-length GRA7 lacking the signal sequence (26C GRA7). Reconstituted liposomes were containing either only PC/PS (80:20) or PC/PS (70:20) plus 10% cholesterol, PI, phosphorylated derivatives of PI, or phosphatidic acid.

(E) Saturation kinetics of 26C GRA7 binding to liposomes. Liposomes (100 μg) were incubated at 37°C for the indicated time (8/1:lipid/rhodamine-GRA7 ratio) before sedimentation. Fluorescence values of GRA7 associated with liposomes are mean ± SD of three experiments.

The Dense Granule Protein GRA7 Tubulates Liposomes via C-Terminal Residues

The above data strongly suggest that constituents secreted by *T. gondii* form the coat present on H.O.S.T. Secreted parasite proteins able to interact with liposomes were identified by immunoblotting from liposomal preparations purified by floatation. All the known hydrophobic GRA (GRA2 through GRA9) were detected in association with the liposomal fractions (Figure 5B).

We therefore investigated the property of these GRA for their ability to deform membrane bilayers. Tubulation assays were performed after immunodepletion of individual GRA from the secreted material (Figure 5C). Similar to control experiments, a massive tubulation of liposomes was observed in the absence of GRA2, GRA3, GRA4, GRA5, GRA6, GRA8, and GRA9, which excludes their necessary involvement in the coat formation. Confirming these results, secreted material from *T. gondii* clones with targeted knockouts of *GRA2*, *GRA5*, or *GRA6* (Mercier et al., 2005) deformed liposomes equivalently to the control (not shown).

By contrast, immunodepletion of GRA7 largely abolished liposome transformation. Confirming this result, material secreted from a *T. gondii* clone with a targeted knockout of *GRA7* showed no liposome deformation. Immunogold labeling on liposomes incubated with total secreted material revealed intense immunoreactivity toward GRA7 along the entire tubule (Figure 5D). No labeling was observed using antibodies against GRA2, GRA3, GRA5, or GRA9 (not shown). In combination, these data strongly implicate GRA7 as a necessary component in tubule formation.

The deduced 236 amino acid GRA7 contains a putative N-terminal signal peptide, 5.5% proline residues, a RGD adhesion motif and a hydrophobic putative transmembrane domain near the C terminus (Jacobs et al., 1998). Like other GRA, GRA7 does not display any conventional lipid binding domains (DiNitto et al., 2003) that might target and remodel membranes. The nature of association with native GRA7 and liposomes was investigated (Figure 6A). The membrane association of GRA7 was not disrupted by treatments capable of releasing peripheral membrane proteins such as high pH or high salt, indicating that it is likely due to a strong hydrophobic interaction. Indeed, GRA7 was solubilized by Nonidet-40, and after Triton X-114 partitioning, GRA7 was found exclusively in the detergent phase. Treatment with the chaotropic agent urea released more than half of the liposome-associated GRA7.

We defined the region of GRA7 required for lipid tubulation. C- or N-deletion mutants of the protein were constructed (Figure 6B) and tested in the presence of large liposomes for generation of tubulation profiles. Native GRA7 (26C GRA7)-induced tubulation was efficient, rapid, and occurred at 4°C, implying that GRA7 alone was able to reconfigure initially flat membranes of appropriate lipid composition into tubules. A C-truncated form preserving all but four residues of the hydrophobic segment of GRA7 (e.g., 5/198 GRA7) efficiently deformed spherical liposomes into tubes. A large deletion of the N terminus of the protein (56C GRA7) only moderately impaired liposome tubulation. However, complete deletion of the hydrophic domain of GRA7 (5/146 GRA7) abolished liposome deformation, implying the central participation of this domain in tubule formation. This observation was confirmed in liposome sedimentation assays (Figure 6C). Both purified GRA7 (26C GRA7) and 5/146 GRA7 remained in the supernatant fraction when centrifuged without liposomes at low speed (10,000 $\times$ *g*). Addition of liposomes to GRA7 induced the pelleting of the protein together with liposomes. By contrast, the 5/146 C-terminal truncation fragment remained in the soluble fraction.

Protein-lipid overlay assays were performed in order to elucidate the specific lipid-affinity properties of the GRA7 (Figure S7). GRA7 interacted with negatively charged lipids, e.g., phosphatidic acid, sulfatides, phosphatidylinositol (PI), and various phosphorylated derivatives of PI. Quantification of GRA7 binding to liposomal membranes of defined lipid compositions confirmed strong binding to liposomes containing 10% phosphatidic acid, PI, PI(5)P, PI(3,4)P_2, PI(3,5)P_2, or PI(4,5)P_2 (Figure 6D). Detectable but weak binding was observed for liposomes containing 10% PI(3)P, PI(4)P, or PI(3,4,5)P_2. No detectable binding of GRA7 was observed to liposomes containing PC/PS and/or cholesterol. Kinetics of GRA7 association with liposomes at 37°C showed an initial linear process before reaching a plateau after 20 min (Figure 6E). GRA7 association with liposomes was saturable at a lipid/protein ratio of 10/1 (Figure 6F). Altogether these results reveal that, like various tubulogenic proteins, GRA7 shows membrane binding properties, with some lipid specificities.

(F) Saturation concentrations of 26C GRA7 binding to liposomes. Liposomes (100 μg) were incubated at 37°C for 30 min at various GRA7 concentrations before sedimentation (lipid/rhodamine-GRA7 ratio shown). Fluorescence values of GRA7 associated with liposomes are mean of two separate experiments.

(G) Immunoblots of secreted proteins after chemical crosslinking. 15 μg/ml of proteins secreted by the parasites (wild-type or *GRA7* KO) were mixed with 1 mM DSP before quenching with 50 mM Tris-HCl (pH 7.5). To cleave the crosslinker, samples were treated with dithiothreitol (DTT). The blots were revealed with anti-GRA7 antibodies at 1/500. The lower band ~18 kDa in wild-type parasites corresponds to a GRA7 degradation product.

(H) Multimerization of 26C GRA7 in the presence of liposomes. GRA7 was incubated with or without liposomes as shown, with 10 mM of the crosslinker EDC, for 0, 15, or 60 min at 37°C. Samples were then prepared for SDS-PAGE analysis. Arrowheads show 26C GRA7 and higher molecular weight products.

(I) Size exclusion chromatography of crosslinked GRA7 complexes. After crosslinking and extraction from liposomes, 0.2 mg/ml of GRA7 material was fractionated by size exclusion chromatography and detected using a standard ELISA protocol. The positions of protein size standards are indicated at the top. Profile data are representative of two independent experiments.

GRA7 Forms Homo-Oligomers in a Lipid-Stimulated Manner

We next attempted to understand the mechanism underlying the liposome constriction mediated by GRA7. Since this protein is abundantly distributed inside the PV, we evaluated if GRA7 has the ability to interact with other parasite proteins in the membrane constriction process. A mixture of material secreted by the parasite was chemically crosslinked before electrophoretic separation and detection with antibodies against GRA7. In the absence of crosslinking, a main band migrated at ~36 kDa corresponding to GRA7 monomer (Figure 6G). Following crosslinking, a form of GRA7 was shifted to ~65 kDa. This band disappeared after complete cleavage of the crosslinking reagent by reduction, suggesting formation of an intramolecular crosslink between GRA7 homo- or heteromeric complexes. No bands were detected in GRA7-deficient parasites. The nature of the protein complexed to GRA7 was identified by MALDI-MS analysis from three separate spots on gels. N-terminal microsequencing and matching to cognate genes by BLAST revealed only peptide sequences from GRA7. This suggests that GRA7 has the ability to form homo-oligomers.

We wanted to determine whether GRA7 has the property to polymerize in the presence of lipids, and thereby influence membrane shape (Figure 6H). In the absence of liposomes, the GRA7 crosslinked to itself as an apparent dimer. However, GRA7 crosslinked into higher-order SDS-resistant oligomers in a liposome-stimulated manner. No oligomerization of 5/146 GRA7 was observed under the same treatments (not shown). These crosslinking data suggest that mature GRA7 may generate bilayer deformation by oligomerizing onto the surface of liposomes. Size exclusion chromatography of GRA7 material extracted from liposomes after chemical crosslinking showed three peaks eluting at volumes corresponding to molecular weights of 37 ± 4 kDa, as well as 67 ± 6 kDa and 105 ± 5 kDa, potentially representing dimers and trimers of GRA7 (Figure 6I). Hence, by associating with and oligomerizing at lipid surfaces, GRA7 constitutes one major molecule forming the electron-dense coat constricting the H.O.S.T.

Absence of GRA7 Impairs Parasite Growth in Nutrient-Depleted Media

H.O.S.T. formation is implicated in endo-lysosome delivery to the PV. Impairing this process should impede parasite growth, based on the hypothesis that endo-lysosomes are delivering essential nutrients from the host to the parasite. We explored this hypothesis, comparing growth of wild-type and *GRA7* knockout parasites under conditions of serum deprivation. Parasite growth was substantially slowed in mutant parasites with a targeted deletion of *GRA7*, when cultivated at lower concentrations of serum (Figure 7A). EM revealed a dramatic vacuolization and loss of organelles in the *GRA7* knockout parasites (Figure 7B).

DISCUSSION

Our current data identify a unique strategy for nutrient acquisition by an intracellular pathogen (Figure 7C). More generally, they illustrate a new mechanism for unidirectional organelle transport and sequestration. Deep MT-based invaginations of the PVM serve as conduits for the transport of host organelles into the vacuolar space. The tubules mediating the host endo-lysosomal delivery system, named H.O.S.T., are then coated by a dense collar of parasite proteins, including GRA7. This coat constricts the tubular conduits, thereby sequestering host organelles in the PV lumen. This model views H.O.S.T. as a concentrated "feeder organelle," where host nutrients are accumulated in juxtaposition to the parasite, allowing maximally efficient acquisition by the intracellular organism.

Usurpation of the Host MT Cytoskeleton

In mammalian cells, stable and long-lived MTs are involved in the maintenance of organelle structure and localization. Dynamic and short-lived MTs are implicated in organelle trafficking (Infante et al., 2000). The MTs beneath the PVM are short, convoluted, and with ends rarely extending to the cytoplasm. They share morphological characteristics with stable MTs and might serve as scaffoldings to preserve the PV structure and maintain the PV in a stationary position near the host nucleus.

The pericentrosomal region is a central checking station for the status of cytoplasmic organelles. It is therefore hereby an optimal localization to control cellular processes under conditions where cellular architecture as a whole is undergoing remodeling, e.g., cell migration or division. The stable juxtanuclear positioning of the PV suggests that *T. gondii* uses the microtubular arrays to acquire its defined subcellular position, strategically positioning the PV in proximity to the majority of mammalian organelles, potential reservoirs of nutrients. Clearly, such usurpation of the host microtubular network results in the manipulation of host cell membrane transport, as exemplified by the mistargeting and local concentration of host endocytic structures to the PV.

Elasticity of the PVM

The invading parasite is surrounded by the PVM, a classical membrane bilayer which is formed rapidly de novo at the time of entry (~10–20 s; Lingelbach and Joiner, 1998). The PVM derives both from the internalization of the host plasma membrane and the coalescence of rhoptry-derived secretory vesicles whose content is discharged into the host cytosol (Hakansson et al., 2001). However, the lipid composition and the nature of protein-lipid interactions in the PVM remain still largely uncharacterized. Our data show that host MTs that are numerous, long, straight, rigid, and uniform in diameter can mediate extensive indentation of the PVM. This implies that the PVM is a fluid and elastic structure, in which free diffusion of lipids and proteins in the plane of the membrane with high diffusion coefficients may occur.

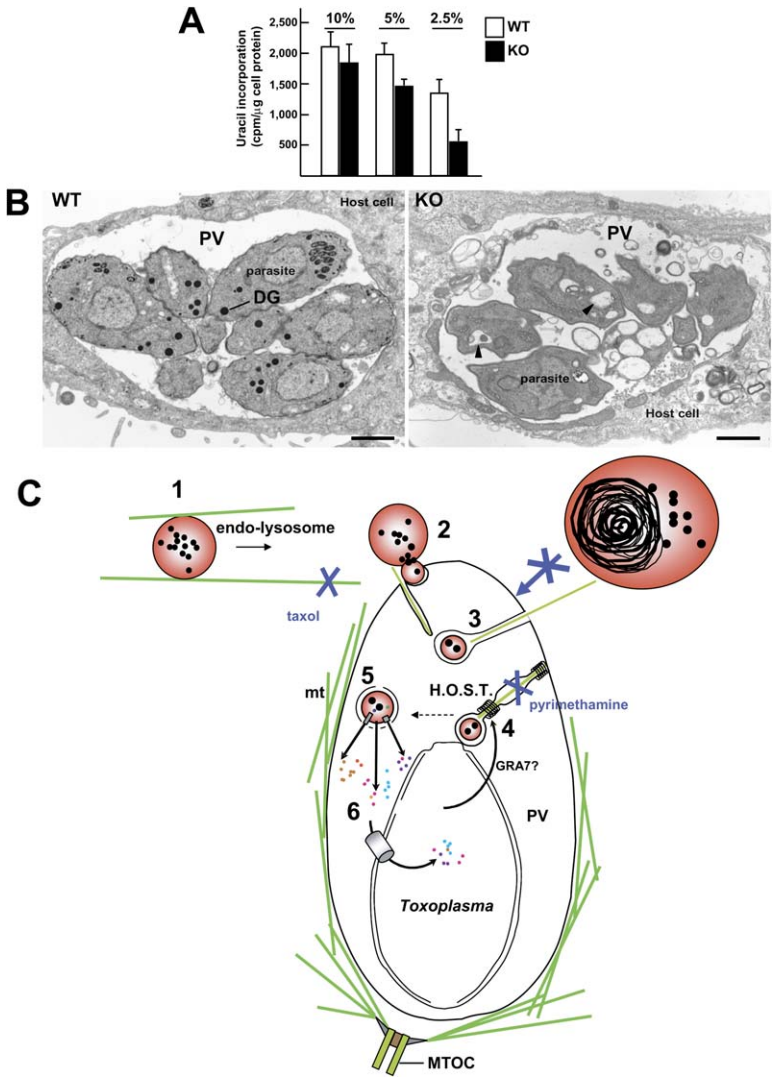

Figure 7. GRA7 Involvement in Nutrient Acquisition and Model on Host Endo-Lysosome Scavenging by *T. gondii*

(A) Uracil incorporation assays on wild-type and *GRA7* knockout parasites 48 hr after incubation in medium containing 10%, 5%, or 2.5% FCS. Data are means ± SD (n = 3).

(B) TEM of wild-type and *GRA7* knockout parasites grown 48 hr in the presence of 5% FCS. Arrowheads show vacuolized structures. The absence of dense core granules (DG) and other electron-dense organelles in the knockout is readily apparent, in comparison to the wild-type parasites. No coated H.O.S.T. was found in the knockout (Ko) PV.
Bars are 0.5 μm.

(C) Hypothetical model. Concomitantly with parasite migration to the host perinuclear area and MTOC association to the PVM, the *Toxoplasma* PV is wrapped in the network of MTs, which indent the PVM. Host endo-lysosomes are translocated to the vicinity of the PV along host MTs (1) and are then closely apposed to the PVM (2) before internalization into the PV through H.O.S.T.-containing host MTs (3). Such conduits are stabilized by secreted parasite coat proteins including GRA7 (4), resulting in PVM constriction and hence sequestration of host endo-lysosomes (5). Intralysosomal molecules produced by hydrolysis can cross the lysosomal membrane via carrier-mediated transporters. Once within the vacuolar space, the molecules can be translocated across the parasite plasma membrane by specific transporters (6). Altogether, these processes lead to a sequestration within the PV of molecules produced by hydrolysis within host endo-lysosomes. Step 1 is inhibited by MT inhibitors, step 3 is blocked by agents that interfere with lysosomal function, and step 4 is inhibited by parasiticidal drugs.

MTs can generate mechanical forces capable of deforming phospholipid membranes. Indeed, artificial liposomes develop tubular projections as encapsulated tubulin assembles (Kaneko et al., 1998). In mammalian cells, deep invaginations in the nuclear envelope are induced by centrosome-associated MTs, leading to nuclear envelope breakdown prior to cell division (Salina et al., 2002). We hypothesize that the polymerization of host MTs can cause PVM tubulation. Formation of PVM tubules requires membrane bending energy, which can depend on the mechanical work generated by MT polymerization but also on the elastic properties of the PVM, reflecting its spontaneous curvature. The formation and stabilization of tubular PVM structures may be achieved by the segregation of various lipids in regions of different membrane curvature, thus providing the membrane with nonhomogeneous elasticity and stabilizing more complex membrane shapes (Kozlov, 2001). The bulk of lipids required for the elongation of tubular PVM extensions may originate from the nanotubules of the TVN in the PV, after local fusion at the site of contact of host MTs with the PVM.

GRA7 as a Membrane Binding Deforming Protein

The electron-dense coat regularly distributed on the H.O.S.T. surface presumably generates mechanical constriction of membranes, causing a local tightening of H.O.S.T. GRA7 is likely responsible for this "pinchase" activity since this protein tubulates liposomes that do not contain any specific intrinsic proteins. Interestingly, GRA7 harbors a PI binding domain. PI recognition domains are commonly implicated in processes such as intracellular trafficking, cellular signalling, and cytoskeletal remodeling. The affinity of GRA7 for lipids and its property to polymerize in a liposome-stimulated manner support the assumption that GRA7 can bind to lipid PVM and constrict the PVM into collared H.O.S.T. GRA7 is abundantly distributed in the PVM. Positive residues of GRA7 may interact with negatively charged lipid membranes, and this

electrostatic attraction may induce a structural change on GRA7 to a more tightly packed and ordered structure. It is plausible that GRA7 is recruited at a certain focus/local point in the PVM, resulting in conformational changes and polymerization in situ, driving PVM tightening. GRA have aberrant membrane-interacting properties. Their transmembrane domains are short, glycine and alanine rich, and have low hydrophobicity coefficents. GRA partition as partly soluble and partly membrane associated both within the parasite and following secretion into the PV. They behave as type I integral membrane proteins during in vitro translation/translocation assays yet are extracted from membranes with sodium carbonate (Karsten et al., 2004). All together, these unusual characteristics of GRA point to the difficulty in intuiting how they can associate and tubulate membranes.

While GRA7 is necessary for H.O.S.T. formation, it may not be sufficient. One clue comes from tubulation assays in the presence or absence of nucleotides. Addition of nucleotides to secreted parasite material resulted in various dramatic conformational changes of liposomes (e.g., vesiculation), in comparison to the situation without added nucleotides (Figure S8). Since GRA7 has no nucleotide binding domains, this result implicates the presence of other candidates in the secreted material that modulate the interaction with lipid membranes. It is possible that such proteins, especially in conjunction with the native lipids on HOST, are required to form the full constriction around the tubule, by generating macromolecular complexes larger than the trimers observed with GRA7 alone. While understanding the details of such complex formation will be of interest, it will not alter the fundamental novelty and importance of the observations made here, and the central role of GRA7 in the process.

Exploitation of the Host Endo-Lysosomal System

The transport of host endo-lysosomes along the PVM tubular extensions and the garroting of H.O.S.T. by the coat formation leads to the sequestration of these host organelles in the vicinity of the parasites. Such sophisticated engulfment of host structures at the PV surface, occurring by invagination of finger-like protrusion of the PVM mediated by MTs, suggests an analogy of the *Toxoplasma* PV with a microautophagosome (Kim and Klionsky, 2000).

The multiple host endocytic structures in the *Toxoplasma* PV can supply exogenous nutrients, e.g., sugars, lipids, amino acids, phosphate, metals, and sulfate, to the resident parasites. The hydrolytic conditions in the PV are confined to the sealed limited environment of H.O.S.T., allowing the release of low-molecular-weight solutes in the local environment while preventing inappropriate autolysis of the PV. The impairment of *Toxoplasma* growth in NPC mutant cells by lack of LDL-cholesterol available for the parasites (Coppens and Joiner, 2003) supports the concept of a parasite dependence of the host endo-lysosomal system for optimal replication.

Most cells acquire nutrients from their environment by a combination of receptor-mediated endocytosis of exogenous macromolecules and by transport of low-molecular-weight solutes. Lacking endocytic activity and endo-lysosomal compartments, *Toxoplasma* relies on transport activities for nutrient acquisition. This reinforces the physiological relevance of H.O.S.T. as feeder organelles in the PV lumen. Genome database analysis (http://www.Toxodb.org/) reveals that *T. gondii* has an extensive repertoire of membrane transporter genes at its disposal. High-affinity nucleoside/nucleobase transporters and hexose transporters located at the parasite plasma membrane have been recently characterized and received attention as putative drug targets.

Of interest, in erythrocytes infected with *Plasmodium,* the PVM extends into the host cell cytosol and to the erythrocyte periphery as a network of tubo-vesicular membranes. This network is conceived as an intracellular transport system acting as a molecular sieve which forms a junction with the erythrocyte membrane, thereby allowing the import of specific nutrients to *Plasmodium* (Haldar et al., 2001). Thread-like extensions of the *T. gondii* PVM into the vacuolar space may reflect the analog of the *Plasmodium* tubulo-vesicular membranes.

EXPERIMENTAL PROCEDURES

Standard methods and specific procedures used to generate the Supplemental Data are described in Supplemental Experimental Procedures.

Chemicals and Antibodies

All chemicals were obtained from either Sigma or Boehringer Mannheim Biochemicals, unless indicated otherwise. Phosphatidylcholine, phosphatidylserine, cholesterol, phosphoinositol, phosphatidic acid, PI(4)P, and PI(4,5)P_2, were purchased from Avanti Lipids. All other phosphoinositides were purchased from Echelon Biosciences. LysoTracker Red DND-99 and Texas red-EGF was from Molecular Probes. Primary antibodies are: rabbit polyclonal anti-GRA3 and mouse monoclonal antibodies to GRA2, GRA4, GRA5, GRA9 (generously provided by J.F. Dubremetz; University of Montpellier); GRA6 and GRA8 (kindly provided by G.E. Ward; University of Vermont); human Lamp-1 (gift from N. Andrews; Yale University); α-tubulin, vimentin and γ-tubulin (Sigma). Polyclonal anti-GRA7 antibodies were produced in rabbits (Covance) using the recombinant GRA7 polypeptide given by Innogenetics.

Parasite Propagation, Mammalian Cell Lines, and Culture Conditions

The tachyzoite RH strain of *Toxoplasma gondii* was propagated in vitro by serial passage in monolayers of HFF (Roos et al., 1994). Mammalian cell lines used included: primary human foreskin fibroblasts (HFF), Chinese hamster ovary (CHO) cells, and VERO cells, which are grown as monolayers (Coppens et al., 2000). The PtK2 cell line stably transfected with YFP-α-tubulin kindly provided by D. Toomre (Yale University).

Labeling of Host Endocytic Structures or Lysosomes

Fluorescence Studies

Cells were incubated for 20 min with the LysoTracker Red according to the manufacturer's instructions or with filipin after fixation. Monolayers of PtK2 cells expressing fluorescent MTs were labeled for 60 min with Texas red-EGF according to the manufacturer's instructions.

Ultrastructural Studies

Infected cells were incubated at 37°C with 0.5 mg/ml of LDL particles or transferrin absorbed to 15 nm gold particles as described (Coppens et al., 1987) before fixation.

Labeling of GRA7 with Rhodamine

Samples containing 1 mg/ml of GRA7 were dialyzed against 100 mM $NaHCO_3$ (pH 9) before incubation with a 4-fold molar excess of rhodamine isothiocynate as described (Holopainen et al., 2000). The amount of rhodamine-GRA7 association with liposomes was determined by light absorption at 580 nm after sedimentation of the complexes.

Crosslinking Assays of GRA7

Samples of parasite secreted material were subjected to crosslinking using the homobifunctional, cleavable crosslinking reagent dithiobis (succinimidylpropionate) (DSP; Pierce) as described (Labruyere et al., 1999) before being analyzed by SDS-PAGE followed by Western blotting using anti-GRA7 antibodies. In another assay, 9 volumes of 4 μg of GRA7 in the absence or presence of 8 μg liposomes were incubated with 1 volume of 1-ethyl-3-(3-dimethylaminoprolyl) carbodiimide hydrochloride (EDC) in HEPES, pH 7.4, 100 mM KCl to achieve final concentrations of 5 and 10 mM crosslinker. The mixture was incubated for 30 min at room temperature, and the samples analyzed on 12% SDS-PAGE.

Size Exclusion Chromatography of GRA7 Complexes

After crosslinking of GRA7-containing liposomes with EDC, GRA7 complexes were extracted with 0.1% saponin and dialyzed in PBS plus 2 mM DTT. Size exclusion chromatography was performed using a Superdex 200 column run by a Pharmacia liquid chromatography controller LCC-500 (Amersham) to analyze proteins in the 10–2,000 kDa range. High- and low-molecular-weight standards were used according to the manufacturer's instructions. Coomassie stain or silver stain was used to detect the eluted standards. Standards and GRA7 preparations were run over the column under identical conditions.

Supplemental Data

Supplemental Data include experimental procedures, eight figures, one table, and supplemental references and can be found with this article online at http://www.cell.com/cgi/content/full/125/2/261/DC1/.

ACKNOWLEDGMENTS

The authors gratefully thank the members of K.A. Joiner laboratory for helpful discussions during the course of this work and the technical staff from the Yale Microscopy Facility. *T. gondii* knockouts of *GRA2/6* or *5* and the strain IFLA/BR/67/PH8 of *Leishmania amazonensis* were kindly provided by Marie-France Delauw and Norma Andrews, respectively. We acknowledge Pietro De Camilli and Khashayar Farsad for their helpful advice for the liposome tubulation assays. The work was supported by grants from the AHA (0230079N) to I.C., from the NIH AI060767 to I.C., AI488443 to K.A.J., and AI45057 to J.C.B. J.D.D. was supported by a predoctoral fellowship from HHMI and by NIH T32 GM07276.

Received: August 4, 2005
Revised: November 29, 2005
Accepted: January 20, 2006
Published: April 20, 2006

REFERENCES

Coppens, I., and Joiner, K.A. (2003). Host but not parasite cholesterol controls *Toxoplasma* cell entry by modulating organelle discharge. Mol. Biol. Cell *14*, 3804–3820.

Coppens, I., Opperdoes, F.R., Courtoy, P.J., and Baudhuin, P. (1987). Receptor-mediated endocytosis in the bloodstream form of *Trypanosoma brucei*. J. Protozool. *34*, 465–473.

Coppens, I., Sinai, A.P., and Joiner, K.A. (2000). *Toxoplasma gondii* exploits host low-density lipoprotein receptor-mediated endocytosis for cholesterol acquisition. J. Cell Biol. *149*, 167–180.

DiNitto, J.P., Cronin, T.C., and Lambright, D.G. (2003). Membrane recognition and targeting by lipid-binding domains. Sci. STKE, re16.

Farsad, K., and De Camilli, P. (2003). Mechanisms of membrane deformation. Curr. Opin. Cell Biol. *15*, 372–381.

Farsad, K., Ringstad, N., Takei, K., Floyd, S.R., Rose, K., and De Camilli, P. (2001). Generation of high curvature membranes mediated by direct endophilin bilayer interactions. J. Cell Biol. *155*, 193–200.

Hakansson, S., Charron, A.J., and Sibley, L.D. (2001). *Toxoplasma* evacuoles: a two-step process of secretion and fusion forms the parasitophorous vacuole. EMBO J. *20*, 3132–3144.

Haldar, K., Samuel, B.U., Mohandas, N., Harrison, T., and Hiller, N.L. (2001). Transport mechanisms in *Plasmodium*-infected erythrocytes: lipid rafts and a tubovesicular network. Int. J. Parasitol. *31*, 1393–1401.

Hall, S., Ryan, K.A., and Buxton, D. (2001). The epidemiology of *Toxoplasma* infection. In Toxoplasmosis: A Comprehensive Clinical Guide, D.H. Joynson and T.J. Wreghitt, eds. (Cambridge: Cambridge University Press), pp. 58–124.

Halonen, S.K., and Weidner, E. (1994). Overcoating of *Toxoplasma* parasitophorous vacuoles with host cell vimentin type intermediate filaments. J. Eukaryot. Microbiol. *41*, 65–71.

Holopainen, J.M., Saily, M., Caldentey, J., and Kinnunen, P.K. (2000). The assembly factor P17 from bacteriophage PRD1 interacts with positively charged lipid membranes. Eur. J. Biochem. *267*, 6231–6238.

Infante, A.S., Stein, M.S., Zhai, Y., Borisy, G.G., and Gundersen, G.G. (2000). Detyrosinated (Glu) microtubules are stabilized by an ATP-sensitive plus-end cap. J. Cell Sci. *113*, 3907–3919.

Jacobs, D., Dubremetz, J.F., Loyens, A., Bosman, F., and Saman, E. (1998). Identification and heterologous expression of a new dense granule protein (GRA7) from *Toxoplasma gondii*. Mol. Biochem. Parasitol. *91*, 237–249.

Joiner, K.A., and Roos, D.S. (2002). Secretory traffic in the eukaryotic parasite *Toxoplasma* gondii: less is more. J. Cell Biol. *157*, 557–563.

Kaneko, T., Itoh, T.J., and Hotani, H. (1998). Morphological transformation of liposomes caused by assembly of encapsulated tubulin and determination of shape by microtubule-associated proteins (MAPs). J. Mol. Biol. *284*, 1671–1681.

Karsten, V., Hegde, R.S., Sinai, A.P., Yang, M., and Joiner, K.A. (2004). Transmembrane domain modulates sorting of membrane proteins in *Toxoplasma gondii*. J. Biol. Chem. *279*, 26052–26057.

Kim, J., and Klionsky, D.J. (2000). Autophagy, cytoplasm-to-vacuole targeting pathway, and pexophagy in yeast and mammalian cells. Annu. Rev. Biochem. *69*, 303–342.

Kozlov, M.M. (2001). Fission of biological membranes: interplay between dynamin and lipids. Traffic *2*, 51–65.

Labruyere, E., Lingnau, M., Mercier, C., and Sibley, L.D. (1999). Differential membrane targeting of the secretory proteins GRA4 and GRA6 within the parasitophorous vacuole formed by *Toxoplasma gondii*. Mol. Biochem. Parasitol. *102*, 311–324.

Lange, Y., Ye, J., Rigney, M., and Steck, T.L. (2002). Dynamics of lysosomal cholesterol in Niemann-Pick type C and normal human fibroblasts. J. Lipid Res. *43*, 198–204.

Lingelbach, K., and Joiner, K.A. (1998). The parasitophorous vacuole membrane surrounding *Plasmodium* and *Toxoplasma*: an unusual compartment in infected cells. J. Cell Sci. *111*, 1467–1475.

Mercier, C., Adjogble, K.D., Daubener, W., and Delauw, M.F. (2005). Dense granules: Are they key organelles to help understand the parasitophorous vacuole of all apicomplexa parasites? Int. J. Parasitol. *35*, 829–849.

Praefcke, G.J., and McMahon, H.T. (2004). The dynamin superfamily: universal membrane tubulation and fission molecules? Nat. Rev. Mol. Cell Biol. *5*, 133–147.

Roos, D.S., Donald, R.G.K., Morissette, N.S., and Moulton, A.L.C. (1994). Molecular tools for genetic dissection of the protozoan parasite *Toxoplasma gondii*. Methods Cell Biol. *45*, 27–63.

Russell, D.G. (1995). *Mycobacterium* and *Leishmania*: stowaways in the endosomal network. Trends Cell Biol. *5*, 125–128.

Salina, D., Bodoor, K., Eckley, D.M., Schroer, T.A., Rattner, J.B., and Burke, B. (2002). Cytoplasmic dynein as a facilitator of nuclear envelope breakdown. Cell *108*, 97–107.

Schwab, J.C., Beckers, C.J.M., and Joiner, K.A. (1994). The parasitophorous vacuole membrane surrounding intracellular *Toxoplasma gondii* functions as a molecular sieve. Proc. Natl. Acad. Sci. USA *91*, 509–513.

Sibley, L.D., Niesman, I.R., Parmley, S.F., and Cesbron-Delauw, M.F. (1995). Regulated secretion of multi-lamellar vesicles leads to formation of a tubulo-vesicular network in host-cell vacuoles occupied by *Toxoplasma gondii*. J. Cell Sci. *108*, 1669–1677.

Sinai, A.P., Webster, P., and Joiner, K.A. (1997). Association of host cell endoplasmic reticulum and mitochondria with the *Toxoplasma gondii* parasitophorous vacuole membrane: a high affinity interaction. J. Cell Sci. *110*, 2117–2128.